Phase-Inversion Applications Beyond Membrane Formation. I. Lithography Films

K. BELTSIOS,[1] E. ATHANASIOU,[1] E. TEGOU,[2] N. KANELLOPOULOS[1]

[1] Institute of Physical Chemistry, NCSR Demokritos, Agh. Paraskevi Attikis, 15310, Greece

[2] Institute of Microelectronics, NCSR Demokritos, Agh. Paraskevi Attikis, 15310, Greece

Received March 1999; accepted November 1999

ABSTRACT: Polymeric films cast from a polymer solution can develop a bulk porosity, if the conditions are favorable for phase inversion (PI), a physical chemical process based on fluid–fluid demixing of which there are two known major variants: wet and dry PI. As the formation of polymeric coatings often involves a polymeric solution or gel precursor, dry or wet PI phenomena may affect the structure formation of the final solvent-free coating. In this article we identify the situations under which lithographic films can develop a PI structure and focus on solid polymer layers undergoing post-casting wet processing. Examples are provided from the wet processing of a fractionated epoxy novolac resin currently used in lithographic patterning. © 2000 John Wiley & Sons, Inc. J Appl Polym Sci 78: 2145–2157, 2000

Key words: phase inversion; polymeric coatings; lithography; epoxy novolac resin; wet silylation

INTRODUCTION

Phase-inversion phenomena are observed when a thin layer of a polymer solution with a typical polymer content in the 5–20% w/w range comes in contact with a fluid that is miscible or partially miscible with the polymer solvent, but not miscible with the polymer. As a result, the solution enters the immiscibility regime of the polymer–solvent–nonsolvent phase diagram (Fig. 1, arrow 1), and eventually a porous polymer membrane structure develops.[1] The pores of the membrane can be isolated or may participate in a continuous network. The diameters of the pores developed in the bulk of the membrane usually belong to one or two size ranges, with 0.5 μm a typical border value between the two ranges.[2] Another type of bulk porous morphology sometimes observed during phase inversion is that of macrofingers. Macrofingers are elongated porous entities with widths in the range of 1–20 μm and a long dimension perpendicular to the membrane surface.[1–4] Although the bulk of the membrane develops a porous morphology, the surface of the solidified polymer develops either a porous structure, more or less similar to that of the bulk (with the exception of macrofingers), or a "skin," that is, a relatively dense arrangement of polymeric particles with interparticle openings in the range of 100 Å or less.[1,2,4]

Within the binodal of Figure 1, the immiscibility regimes α, β, and γ are shown. Regime α, where nucleation and growth (NG) of liquid-rich droplets can take place, tends to yield films with isolated convex pores and porosities usually less than 25%. In regime γ, where spinodal decomposition can take place, the film porosities tend to be higher than those of regime α. In addition, regime γ pores have

Correspondence to: K. Beltsios.

Journal of Applied Polymer Science, Vol. 78, 2145–2157 (2000)

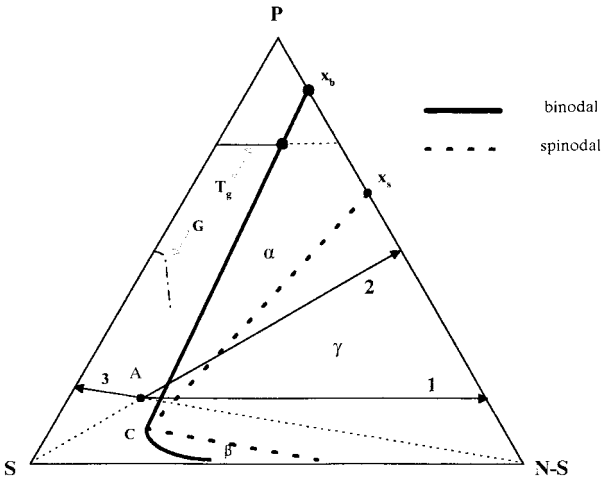

Figure 1 Polymer (P)–solvent(S)–nonsolvent (N-S) phase diagram and PI; volume fraction–based compositions. Phase separation regimes: α (NG of polymer-poor droplets), β (NG of polymer-rich droplets), γ (SD). Arrow 1: Overall film composition during wet PI with no overall change of fluid volume. Arrow 2: Overall film composition during dry PI with S much more volatile than N-S. Arrow 3: Prevention of dry PI by choosing a solvent less volatile than the nonsolvent. x_b: trace of binodal line, x_s: trace of spinodal line. Locations of T_g line with metastable (dotted) extension and gel (G) line are also indicated.

contours of alternating positive and negative curvature and tend to be interconnected.[2]

A dry variation of the PI process[5] is observed when a polymer is dissolved in a mixture of a volatile solvent and a less volatile nonsolvent and, subsequently, a layer of the polymer solution is left to dry. During drying the more volatile solvent will evaporate faster than the nonsolvent, thus eventually bringing the drying solution into the immiscibility regime of the polymer–solvent–nonsolvent phase diagram and creating conditions favorable for the formation of a PI structure (Fig. 1, arrow 2). The formation of a dry PI structure can be prevented if a solvent much less volatile than the nonsolvent is chosen (Fig. 1, arrow 3).

Also shown in Figure 1 is the glass-transition temperature (T_g) line[2b,6] and the gel (or, dissolution) line.[7] The T_g line need not be exactly parallel to the solvent–nonsolvent axis. Pores formed within a matrix having a composition lying above the T_g line tend to be mechanically stable. However, pores may on various occasions eventually stabilize, even if at the time of pore formation the matrix composition lies below the T_g line but is still above the gel line. The gel line of Figure 1 is a line of single-phase compositions. The mechanical response of a material with a composition lying above the gel line will be that of a solid, at least over short times. Below this line, the polymer will dissolve. For some polymer/solvent systems, including the cellulose acetate/acetone and cellulose acetate/dioxane[7] and Epikote 164 (a commercial epoxy novolac)/propylene glycol methyl ether acetate (PGMEA) pairs, the gel line meets the polymer/solvent axis at approximately a 1:1 composition, though, conceivably, this point can lie much closer to the pure solvent apex, while the polymer/solvent/nonsolvent ternary phase diagram retains the generic features of Figure 1. As dissolution of a polymer is often a rather complex process and more than one layer forms between the bulk of the polymer and the fluid phase,[8,9] additional compositional boundaries, defining regions (e.g., rubbery regime) with different mechanical properties, and diffusion coefficients may exist between the T_g and gel lines shown in Fig. 1. It may be assumed that in the general case the course of those additional lines will fall between the courses of the T_g and gel lines.

In addition to the situation represented by arrow b in Figure 1, dry PI may be observed if, for a given polymer, two fluids exist that separately behave as moderate solvents or nonsolvents, but their mixture is fully miscible with the polymer within a range of ratios. Miscibility of this type (known as cosolvency[10]) is possible when, for example, one fluid is more polar and the other fluid is less polar than the polymer. In terms of PI, a difference in the volatility of the two moderate solvents or nonsolvents can also create dry PI phenomena during the drying of the solution (Fig. 2).

PI-related phenomena may also be observed for thermally quenched binary polymer solutions.[11] Finally, we note that demixing inside the binodal (or inside the spinodal) is not the only polymer–solvent demixing route that can generate porosity in a polymer. Thermal quench of a binary polymer solution as a means to form a porous membrane with or without the involvement of demixing inside the binodal or spinodal has been explored by Lloyd et al.[12] An example of a phase-separation route leading to stable porosity in a polymer structure without the involvement of demixing within a binodal is provided by the 0.5 μm pores developed in a propylene film through a eutectic solidification route.[13] Nevertheless, such phase

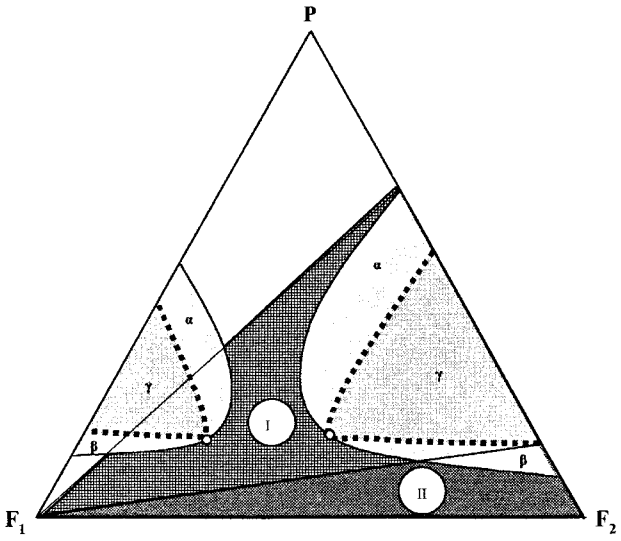

Figure 2 Ternary phase diagram of a polymer, P, partially miscible with two fluids (F_I, F_{II}); volume fraction–based compositions. If F_I is much more volatile than F_{II}, then the compositions of shadowed area I may lead to porous films through dry PI. If F_I is moderately more volatile than F_{II}, some of area I and some of area II compositions may yield porous films through PI. Comparable volatility of F_I and F_{II} will often lead to compact or near compact films.

separation modes are outside the scope of this work.

In this and a subsequent work,[14] we will examine the potential role of PI phenomena during the processing of polymeric coatings other than free-standing membranes. Such coatings are usually formed or, more generally, processed through routes involving the drying of a polymer–fluid layer, and, consequently, we will focus primarily on phenomena related to dry PI. Nevertheless, wet PI or complicated processing sequences, which include PI-related steps, may also be encountered in some cases. As an example of the former, a PI structure may develop if a drying layer derived from a lower alcohol, ketone, or ether solution of a non-water-soluble polymer comes in accidental contact with water while a substantial amount of solvent is still present in the film. In general, water capable of PI induction may have the form of bulk fluid, environmental humidity, or substrate moisture.

Here we explore the relevance of PI to lithographic film processing, while in Part II we will turn our attention to paint and primer coatings and protective layers of biological tissues. Under usual circumstances, PI structure formation is undesirable in the first two cases, though it may be desirable in the third case.

Currently, the optimization of lithographic processing is predominantly done in an empirical manner. The prevalence of empirical optimization may be attributed to two main factors: (1) the fast pace of microelectronics evolution, and (2) difficulties in the theoretical approach of the issues involved in processing—lithography involves long sequences of non-steady-state steps with multicomponent materials and dimensions belonging to the sometimes-difficult-to-tackle-theoretically mesoscopic (submicron) scale. An early demonstration of the use of physical chemistry concepts in lithography processing is the influential work by Novembre et al.[15] This work dealt with the selection of solvents and nonsolvents for the developer–rinse pair for a negative resist in terms of the solubility parameter and molecule size considerations. In the last decade the physical chemistry and the chemistry of the most important type of solution processing—the dissolution mechanism of novolac-diazoquinone resists—has also received considerable attention.[8a,16]

Lithography and PI Processes

Basic Considerations

PI phenomena can affect the structure of a lithographic polymer film in at least three general types of situations. For the first type, encountered during original film casting from solution, we will identify the processing situations most favorable for PI phenomena.

The second type of situation is encountered during postcasting solution processing of the lithographic polymer film. Such processing may aim, for example, at selectively impregnating with a desirable agent the noncrosslinked areas of a crosslink-patterned but not developed polymer film. In the same example, the agent that's been introduced (a silylating compound, for example) can protect the noncrosslinked domains against oxygen plasma etching and thus allow for the *dry* development of a lithographic pattern by selective oxidation of the crosslinked, nonimpregnated portion of the pattern.[17] Although wet silylation faces the alternative of dry silylation and at this point is a specialized lithographic process, our relevant considerations are pertinent to any postcasting impregnation of a thin noncrosslinked film or portion of a polymeric film. In particular, we discuss from the dry PI point of view and with

the help of a generic polymer–solvent–nonsolvent phase diagram, the soaking with a solvent–nonsolvent fluid of a thin noncrosslinked polymer film and the subsequent drying of this film. Experimental work is based on Epikote 164 (EPR), an epoxy resin used in lithography both as described above[18] and also as a negative resist.[19] EPR is cast in thin compact films by spin-coating and is subsequently subjected first to postcasting soaking in various solvent–nonsolvent mixtures and then to drying. As neither the crosslinked areas nor the presence of a silylating agent are relevant to the PI issue in discussion, the related steps are excluded from EPR processing, and our findings are independent of the particulars of the wet silylation process.

Another important point is the thickness of the polymeric film. In the case of PI studies pertinent to polymer membrane formation, the amount of polymer employed corresponds to a compact film thickness of some tens of microns, while in the case of microelectronics processing, the film thickness is in the 1 μm range. On the other hand, as PI pores often grow at a minimum distance of 0.1–0.3 μm from the top surface of the film, a film thickness of 1 μm or less may not allow the unambiguous attribution of certain film structure trends to PI. In particular, PI consequences may be erroneously perceived as a demonstration of excessive dissolution strength of a particular solvent–nonsolvent mixture or a case of poor polymer film adhesion on the substrate. Hence, for tests aiming at the identification of the operation of a PI process, a film thickness in the range of 1.5–5 μm may be preferred.

The third general type of lithography processing where PI consequences may be encountered is that of developing and rinsing certain negative resists. Although a solvent treatment followed by a nonsolvent treatment resembles *wet* PI processing, the presence of crosslinks makes potential PI structural consequences relatively subtle and also difficult to interpret unambiguously.

Finally, we note that channels with a width in the 0.2 μm range and running near perpendicularly to the membrane surface for approximately a micron have been observed in some cases of membrane wet PI.[20] Hence, at least in the case in which a lithography step is related to wet PI, this channel formation process should be considered as a potential source of structural inhomogeneities.

PI and Film Casting from Solution

When a lithographic film is cast from solution, PI phenomena can be observed during the casting or drying step. During the casting step a polymer solution based on a solvent miscible with water [e.g., methyl ethyl ketone (MEK)] may admit some minute quantity of water from a humid environment. However, unless a thin layer of the solution is left to stand in the air for a long time and thus absorb a significant amount of water, spin coating is sufficiently fast to prevent the appearance of PI structural consequences.

Nevertheless, *dry* PI is a possibility, provided the film is cast from a single-phase solution that contains an appreciable amount of a nonvolatile nonsolvent. Dry PI is also possible when the film is cast from a single-phase solution containing two moderate or poor polymer solvents, that is, solvents that individually do not mix with the polymer in all proportions but are still able, when combined in a particular range of ratios, to mix with the polymer at all fluid–polymer proportions.

The first of the above cases corresponds to the standard form of dry PI. It may be encountered in film casting, if at this point of processing an agent of a polarity substantially different from that of the polymer needs to be incorporated in the polymer mass and, consequently, the solvent quality is adjusted accordingly. The PI problem can then be avoided by replacing, for example, the second fluid with a lower molecular weight member of its family.

The second of the above cases may be encountered when, for example, an alternative to an undesirable single solvent is sought. The essentials of this case are depicted in Figure 2.

It must be noted than in all of the above cases, even if phase diagram considerations suggest that the system is susceptible to PI phenomena, a fast drying step (such as spin coating) will usually prevent the occurrence of PI-related gross structural inhomogeneities. This is especially true when the intra–"miscibility gap" portion of the drying route crosses primarily regime α, as fast drying (e.g., by spin coating) may compete successfully with nucleation. On the other hand, in the case of extensive crossing of regime γ, some PI-related structural features, such as pore traces or at least fluctuations in material density, may be expected, even if drying is fast, as spinodal decomposition (SD) requires no incubation period (see also below).

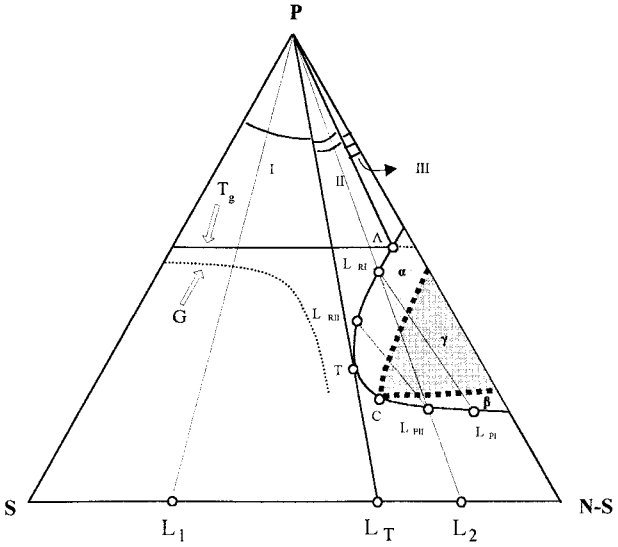

Figure 3 Soaking of a polymer (P) film with a solvent–nonsolvent (S–N-S) mixture. Line PL_T is tangent to the binodal at T, while $\lambda_1 > \lambda_T > \lambda_2$. L_{RI}, L_{RII}, L_{PI} and L_{PII} points and regime I, II, and III fluid compositions, as discussed in the text. T_g line meets the binodal at Λ.

As for the possibility of PI phenomena during original film casting, it is worth noting that much of the large current interest in microelectronics favors polymer–solvent systems based on solvents that are mild in terms of health and environmental consequences. As such solvents are often miscible with water, air-humidity- or substrate-moisture-induced PI should receive some consideration. On the other hand, it is obvious that PI induction through humidity or moisture adsorption will not be possible if lithography eventually excludes all processes other than water-based and dry steps.

PI and Film Impregnation and Drying

A generic phase diagram pertinent to impregnation and drying processing is shown in Figure 3. PL_T is a line tangent to the binodal and drawn from the 100% polymer apex, while λ_T is the solvent–nonsolvent ratio corresponding to L_T. Line PL_1 corresponds to a $\lambda_1 > \lambda_T$ and line PL_2 corresponds to a $\lambda_2 < \lambda_T$. During soaking of the polymer film with a solvent–nonsolvent liquid having a λ_1 composition, the membrane will adopt compositions along the PL_1 line, while line PL_2 will be followed if the fluid has a λ_2 composition.

Line PL_2 crosses the polymer-rich side of the binodal at L_{RI} and the polymer-poor side of the binodal at L_{PII}. Points L_{RI} and L_{PII} and corresponding tie lines also define points L_{RII} and L_{PI} on the binodal. The relative position of the L_{RII} and L_{PI} points with respect to a PL line that indirectly defines them may be that shown in Figure 3 or the inverse, depending on the value of λ and the slope of the tie lines.

If a polymer is soaked in a fluid of λ_2 composition for a sufficiently long time, the film layer will develop a composition that will gradually drift from L_{RI} and L_{RII}. On the other hand, for short soaking times, the lower portion of the film will exhibit concentrations along the PL_{RI} line. If the solvent is much more volatile than the nonsolvent, during drying the overall composition of any point of the film will follow the extension toward the polymer–nonsolvent axis of the line connecting the pure solvent apex with the point of composition at the end of soaking. As an example, if L_{RII} corresponds to the composition of a portion of the membrane at the end of the soaking period, then during drying this portion of the membrane will first cross regime α, but will also spend some time in regime γ.

As noted earlier, phase separation inside regime γ starts instantaneously and often yields a bicontinuous structure. Nevertheless, although phase separation in regime γ does not require any type of incubation period (e.g., nucleation), a large gradient in composition and large polymer-rich and polymer-poor domains may take some time to grow. By gradually reducing the difference in volatility between the nonsolvent and the solvent, the line of film compositions adopted during drying can be made to cross mainly the α regime. Finally, if a nonsolvent *more* volatile than the solvent is used, then the film can dry without adopting any compositions belonging to the two-phase portion of the ternary phase diagram.

If a polymer is soaked in a fluid of composition λ_1 for a sufficiently long time and if in addition the overall composition is below the gel line, then the whole film will eventually dissolve. The composition of the soaked but not dissolved portion of the film during drying can be traced as was done in the λ_2 case. For a solvent that is more volatile than the nonsolvent, the most soaked but not dissolved portion of the film will also be the strongest candidate for the development of a continuous pore structure, typical of regime γ of the phase diagram.

The rate of dissolution may be followed through the final film thickness (x_f) or the loss of material. As the loss of material is actually mon-

itored as a change in volume, after porosity is subtracted, changes in the density of the bulk material as a result of soaking cannot be taken into account independently of the loss of material. The intensity of PI consequences can be conveniently monitored by the level of porosity. We note, however, that the porosity level is the easy-to-measure outcome of a complicated sequence of processes.[2] For example, within the same film, different layers may exhibit different levels and types of porosity. For a single-phase starting material and regime α drying, if *long routes near the binodal* generate a number of pores, then *short routes near the binodal* may generate fewer and smaller pores, and *long routes closer to the spinodal* may generate numerous small- or moderate-size pores and, possibly, maximum porosity.

The following three main soaking-step regimes may now be defined on the basis of the λ value: regime I: $\lambda < \lambda_T$, regime II: $\lambda_T < \lambda < \lambda_\Lambda$, regime III: $\lambda_\Lambda < \lambda$. For the same moderate soaking time and original sample thickness (x_o) and assuming that the T_g and gel lines follow the course shown in Figure 3, the following trends in the rate of dissolution and intensity of PI consequences are possible:

For regime I, as λ becomes smaller, both x_f and the level of porosity (ε) may tend to increase.

For regime II, as λ becomes smaller: (a) x_f may tend to decrease, and ε may tend to decrease as well. Nevertheless, a necessary condition for such tendencies to be observed is a degree of soaking such that a significant portion of the film has a composition near the binodal and dissolution has progressed to some extent. On the other hand, the opposite tendencies may be observed if at the end of soaking most of the film has compositions far from the binodal.

Finally in regime III, a metastable extension of the T_g line will allow the process of dissolution to proceed through wet-PI-type intermediates within a glassy matrix. As a result, PI precursor structures formed during soaking may be preserved during drying, and this may result in a sudden increase in film thickness and level of porosity compared to the low λ side of regime II (Table I).

Dissolution in regime I will proceed without a PI intermediate step. While such an intermediate is possible for both regimes II and III, a sufficient guarantee that the PI structure can be (meta)stable exists only for regime III. Nevertheless, some limited time stability of a PI intermediate to dissolution may be possible, as long as $\lambda < \lambda_{\Lambda'}$ ($< \lambda_{\Lambda'}$), where Λ' will be the point where the binodal meets the first of the characteristic lines lying potentially between the T_g and gel lines. The formation and especially the survival of PI precursors formed during the soaking period is highly undesirable, as fast drying may prevent further growth but has no effect over the, prior to drying, biphasic structure evolution. However, it may be noted that an increase in temperature raises the T_g line and, in the case of the upper critical solution temperature behavior, also causes the biphasic regime to shrink. Hence, it may be possible to control PI morphology originating in the soaking period through judicious variation of temperature and possibly soaking time as well.

Table I Expected PI Structural Trends Following Soaking and Drying of a Lithography Film

Regime	For:	x_f Trend	ε Trend
I	$\lambda \downarrow \Rightarrow$	$x_f \uparrow$	$\varepsilon \uparrow$
II	$\lambda \downarrow \Rightarrow$	$x_f \downarrow$ [a]	$\varepsilon \downarrow$ [a]
III	$\lambda \downarrow \Rightarrow$	$x_f > x_{f,\mathrm{II,\ low}\ \lambda}$	$\varepsilon > \varepsilon_{\mathrm{II,\ low}\ \lambda}$

[a] Leading tendency.

Finally, as L_{RI} and L_{RII} (Fig. 3) do not in general coincide, it is possible that for a limited range of fluid compositions, the two points may belong to different sides of the λ_Λ (or $\lambda_{\Lambda'}$) line. Another potential complication is the deviation from λ lines during *single-phase* soaking. Such deviations will reflect differences in the diffusion coefficients of the solvent and nonsolvent and in border cases may bring the film in a soaking regime different from that suggested by the phase diagram and the soaking-fluid λ_Λ value. For members of a homologue series (either of the solvent or the nonsolvent component) the smaller molecules may favor larger drifts.

All suggested trends of the *monotonic* change of x or porosity as a function of λ are a rough guide only. Deviations from these trends, at least for a limited range of λ, can be easily observed, depending on the details of the phase diagram and/or the soaking time. For example, if the T_g line exhibits an upward drift with increasing nonsolvent fraction, this drift may interfere with the suggested regime I monotonic increase of x_f with decreasing λ. Also, a possible drop in the diffusion coefficients of the fluid components with decreasing λ may interfere with the monotonic decrease of x_f with decreasing λ, suggested for regime II.

When the solvent is water-miscible, even if the volatility of the nonsolvent excludes the possibility of *dry* PI, some PI interference through humidity adsorption is possible, at least in principle. Incidentally, it must be noted that the current tendency in film-formation technology to move toward processing with milder solvents, some of which are water-miscible, also increases the chance for PI phenomena during generic film processing from solution: humidity, accidental contact with water before drying, moisture originating from the substrate (especially a substrate with some porosity or even surface roughness) may affect the quality of the polymer–substrate interface.

PI and Negative Resist Processing

When the final lithographic pattern is a result of the preservation of the crosslinked polymer film regimes (a case of negative resist), the potential PI consequences of postcrosslinking processing involving a solvent–nonsolvent mixing will be more subtle than those described in the previous section.

An example is offered by the rinsing of a solvent-soaked film with a nonsolvent. The crosslink density of the soaked (swollen) film places an upper limit at the length scale that phase separation can take place. This limit can be estimated through consideration of the typical crosslink-to-crosslink distance in the random coil and the fully stretched chain configurations. A simple calculation suggests that for a crosslink density of 1%, PI can not introduce inhomogeneities at a scale larger than the equivalent length of $100^{1/2}$ to 100 bonds. Hence, for a crosslink density of 1%, PI inhomogeneities cannot be encountered beyond the 10^1 to low-10^2 Å scale. Further, any pores or density fluctuations of PI origin will survive only if the glass-transition temperature of the film resin is above room temperature and also above any subsequent processing temperature. On the other hand, if crosslinking is grossly inhomogeneous by itself (e.g., at a scale of 0.05–0.1 μm), then the structural consequences of soaking and rinsing will depend both on the access of these domains to a free surface and the manner of crosslinking. Examples of potential PI structural features near the bottom boundaries or sidewalls of a crosslinked domain are depicted schematically in Figure 4. Regarding prevention, the solvent–nonsolvent volatility considerations of the previous section apply here as well.

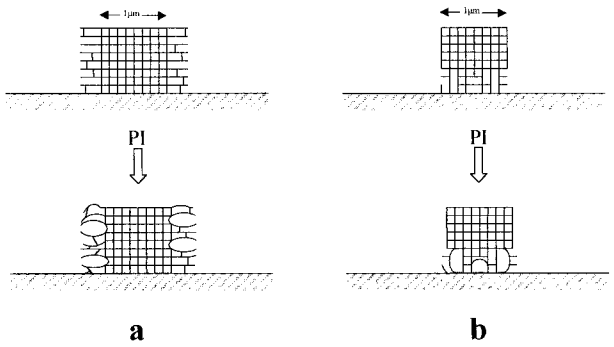

Figure 4 Schematic of PI possibilities in the inhomogeneously crosslinked boundaries of a crosslinked domain: (a) development of sidewall PI inhomogeneities, (b) development of PI inhomogeneities at the bottom of a domain. In each case, the bulk of the domain is densely crosslinked, while the chains of the boundaries may or may not be ultimately attached to the dense network and may or may not be occasionally bridged. Pockets in the PI structure represent low-density areas. T_g is higher than all temperatures of processing subsequent to PI.

EXPERIMENTAL

Epikote 164, a cresol epoxy novolac resin with T_g = 54°C,[18c] was fractionated (M_w = 2100, M_n = 1200) according to a procedure published elsewhere[21] for a similar material. The fractionated product was dissolved in PGMEA and spin-coated on a silicon wafer at a thickness in the 3.5–4 μm range. After drying, the film was dipped in a large excess (1:5,000 volume ratio) of a solvent–nonsolvent mixture for 5 min. Finally, the excess fluid was removed mechanically, and the sample was exposed to the air to dry. The above procedures were followed for the following samples:

(1) A series of samples soaked in PGMEA–alkane (solvent–nonsolvent) mixtures was prepared for the alkanes *n*-decane and *n*-dodecane for the following solvent–nonsolvent ratios (v/v): 40/60, 30/70, 25/75, 20/80, 17/83, 14/86 and 07/93.
(2) Samples soaked with 20/80 solvent–nonsolvent mixtures were prepared for the PGMEA–isooctane (2,2,4-trimethylpentane) and MEK–*n*-decane solvent–nonsolvent pairs.

In addition, PGMEA–*n*-dodecane samples soaked with 20/80 and 07/93 mixtures were prepared as above, with the exception of the final drying step, which was accelerated by sample

Table II Structure of Air-Dried EPR Films Soaked for 5 Min in a PGMEA–*n*-Decane Mixture

	Sample Number						
	1	2	3	4	5	6	7
λ	40/60	30/70	25/75	20/80	17/83	14/86	07/93
x_o (μm)	3.95 ± 0.05	3.95 ± 0.05	3.95 ± 0.05	3.95 ± 0.05	3.95 ± 0.05	3.95 ± 0.05	3.95 ± 0.05
x_f (μm)	2.6 ± 0.2	3.20 ± 0.05	3.3 ± 0.05	3.45 ± 0.10	3.95 ± 0.05	3.85 ± 0.05	3.65 ± 0.05
x_p (μm)	0.5–1	1	1 + 1	1	1	—[a]	—
Pore diam. (μm)	0.1–0.3	0.3–0.4	0.1–0.2 + 0.8–1.0	0.5–0.7	0.1–0.2	—[a]	—
ε_{local} (%)	1–2	5	5% + 5%	10	2	—[a]	0
ε (%)	0.5	1.5	3	3	0.5	0	0
Loss (%)	34	20	19	15	0.5	2.5	8

[a] Pore traces present.

spinning on a spin coater and subsequent nitrogen blast.

Finally, 1.5-μm-thick samples cast on a Si wafer were dipped for 2 min in 93.7/6.3 and 20/80 methanol–*n*-decane mixtures, while drying was accomplished by exposure in the air. The first of the two mixtures was a single-phase fluid, while for the second biphasic mixture the sample was in direct contact with the lower, methanol-rich phase. Finally, the wet films were dried by exposure to the air.

Empirically optimized actual wet silylation processing conditions[18a] were:

EPR film thickness: 0.5–1 μm; soaking bath: PGMEA–*n*-decane–silylating agent [$Si(CH_3)_2Cl_2$]: 15/80/05 (v/v/v); soaking time: 2 min, accelerated drying by nitrogen gun. The soaking fluid composition may be described as having a 15% (v/v) PGMEA content or a 15.8/84.2 PGMEA–*n*-decane v/v ratio. No pores could be detected by SEM in the final product, though a fine structure at the 10–30 nm scale was often present.

In terms of volatility, the various solvents and nonsolvents used were ordered as follows (boiling points in parenthesis): *n*-dodecane (216.2°C) < *n*-decane (174°C) < PGMEA (145°C) < isooctane (98–99°C) < MEK (80°C) < methanol (64.7°C). It should be noted that methanol may be inappropriate for actual silylation processing, as it can react with certain silylation agents (e.g., dichlorodimethylsilane), but no such interference was possible in our silylation agent-free processing.

Porosities (ε) were determined by scanning electron microscopy observation of cross-sectioned samples. The original and final film thicknesses (x_o and x_f) were determined by a Dektak IIA instrument.

RESULTS AND DISCUSSION

The results for air-dried PGMEA–alkane–processed EPR samples appear in Table II (alkane = *n*-decane) and Table III (alkane = *n*-dodecane).

Table III Structure of Air-Dried EPR Films Soaked for 5 Min in a PGMEA–*n*-Dodecane Mixture

	Sample Number						
	1	2	3	4	5	6	7
λ	40/60	30/70	25/75	20/80	17/83	14/86	07/93
x_o (μm)	3.62 ± 0.02	3.62 ± 0.02	3.62 ± 0.02	3.62 ± 0.02	3.62 ± 0.02	3.62 ± 0.02	3.62 ± 0.02
x_f (μm)	2.0 ± 0.3	3.7 ± 0.3	4.05 ± 0.05	4.10 ± 0.10	3.60 ± 0.05	2.4 ± 0.3	3.9 ± 0.2
Pore diameter (μm)	0.1–0.3	1.0–1.2	0.3–1.2	0.3–0.7	0.2–0.6	0.2–0.7	0.2–2.0
ε (%)	2–3	8–10	13–15	10–11	6–8	4	22–25
Loss (%)	46	7	4	0	7.5	36	17

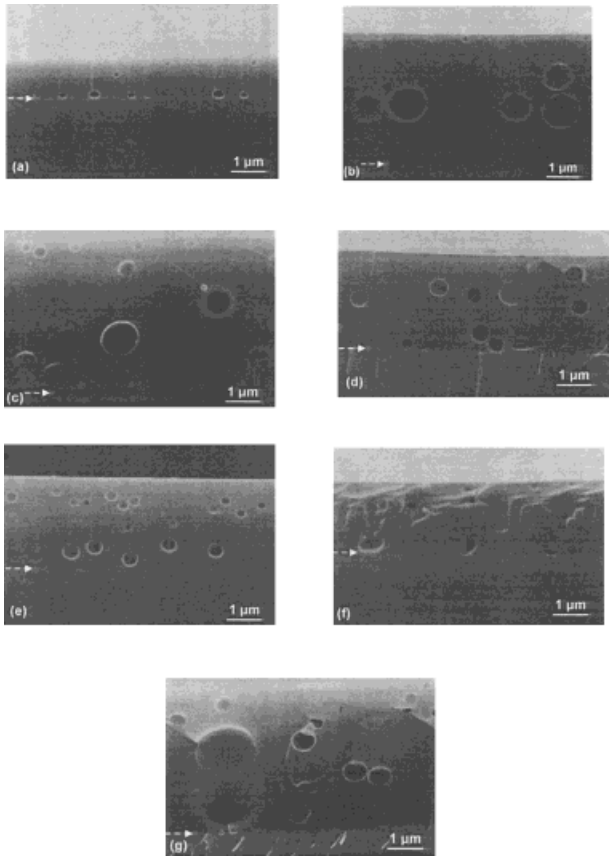

Figure 5 Cross sections of EPR film on Si wafer after soaking with a PGMEA–*n*-dodecane mixture with the following compositions (v/v): (a) 40/60, (b) 30/70, (c) 25/75, (d) 20/80, (e) 17/83, (f) 14/86, (g) 07/93. Pores reach the bottom for samples a, d, f, and g and almost reach the bottom for samples c and e. For sample b the lower third of the sample is free of pores. Horizontal arrows indicate the location of the polymer–Si interface. x_o = 3.6 μm. All samples are air-dried.

Selected structural features for all types of EPR systems examined appear in Figures 5–11. In the case of *n*-decane as the nonsolvent the porosity was localized in one or two bands with a thickness (x_p) of about of 1 μm. The local porosity ($\varepsilon_{\text{local}}$) within the porous band(s) is listed in Table I.

Features common to practically all samples examined include standard PI features such as fractionated low molecular weight,[22] spherical entities on the surface of the final product, and a 0.1–0.2 μm thick skin[1,2] that was often detachable.

With the exception of the 07/93 samples (see below), the PGMEA–*n*-dodecane series led to much higher overall porosities than the PGMEA–*n*-decane series, as expected on the basis of our nonsolvent volatility considerations previously explained.

Table III data on the maximum in porosity (ε) and minimum in material loss suggest that λ_T corresponds to a fluid composition such as 25/75 or 20/80 for the PGMEA–*n*-dodecane system. Table II data suggest that λ_T for the PGMEA–*n*-decane system compared to that for the PGMEA–*n*-dodecane system was shifted by approximately one square toward lower λ values. For the PGMEA–*n*-dodecane system, samples 1 and 2 belong to regime I, samples 3 and 4 correspond to the $\lambda \sim \lambda_T$ range, samples 5 and 6 belong to regime II, and sample 7 belongs to regime III. None of the examined PGMEA–*n*-decane samples belongs to regime III, and this difference between the *n*-decane and *n*-dodecane systems may result from a

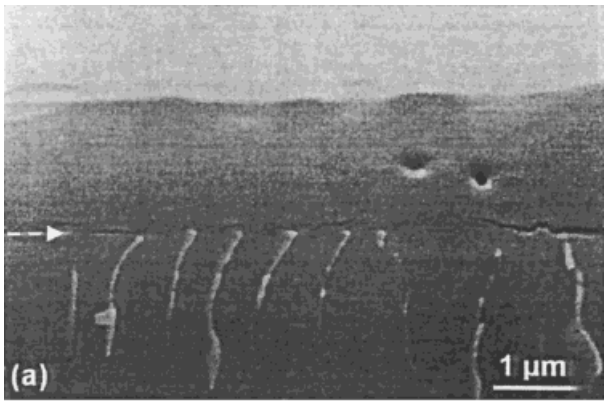

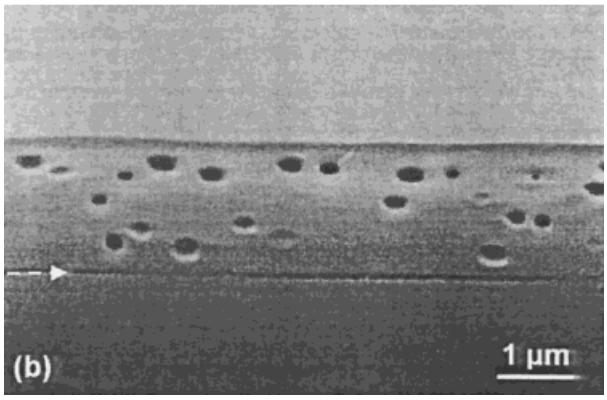

Figure 6 Cross sections of quick-dried EPR films soaked for 5 min in a PGMA–*n*-dodecane (a) 20/80 and (b) 07/93 mixture. Nucleation is rare in the case of (a) but very extensive in the case of (b), as the latter nuclei originate from the soaking period.

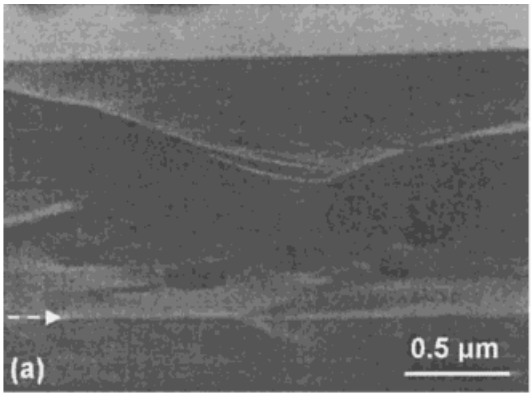

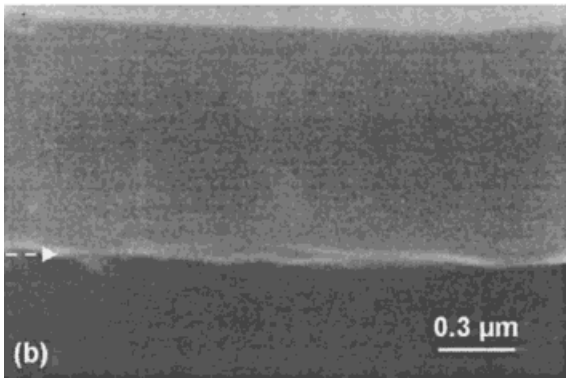

Figure 7 Cross sections of an EPR film soaked for 5 min with a PGMA–alkane 20/80 mixture and subsequent air drying. Compared with Figure 5 (d), showing the structure for alkane = *n*-dodecane, sample a (alkane = *n*-decane) exhibits fewer pores and sample b (alkane = isooctane) shows practically no porosity.

higher location of the T_g line and/or, in the case of the PGMEA–*n*-decane system, to a more narrow biphasic regime. The suggestion that the 07/93 sample of Table III belongs to regime III can be tested through examination of the effect of accelerated drying for samples 20/80 and 07/93 of Table III. The results are shown in Figure 6. Accelerated drying has suppressed substantially the PI structure only in the first case, as the nucleation and portion of the growth of the PI structure of the second case forms primarily during soaking. Still, there is a large difference in porosity between the quickly and slowly dried 07/93 samples (4% vs. 22–25%). Our data suggest the following picture: The slow step of nucleation plus a small portion of growth are accomplished during soaking and lead to an overall porosity $\simeq$ 4%. Growth itself may be faster than nucleation but not fast enough to compete with accelerated drying. The difference in the porosity of the two Figure 6 samples (22–25% compared to 4%) reflects primarily the growth accomplished during air-drying. Nevertheless, it can be stated that a regime III sample can develop a substantial level of undesirable porosity, regardless of the drying rate. In the case of the fast-dried 20/80 PGMEA–*n*-dodecane sample, thickness measurements indicate that that the compact-looking film has suffered an overall lowering of density on the order of

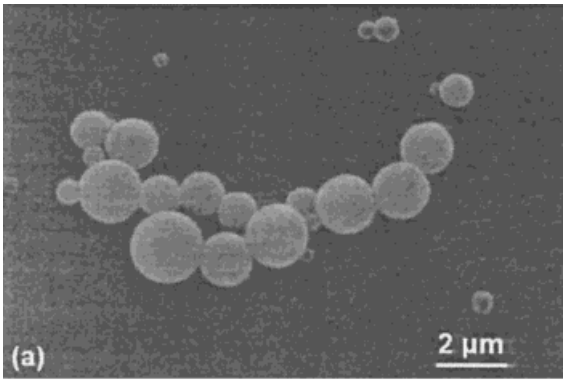

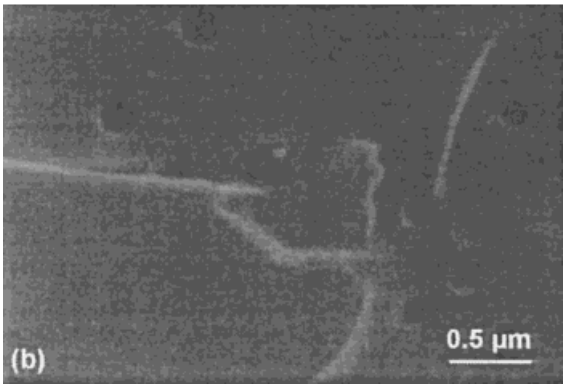

Figure 8 Surface spherical entities and a skin are PI features common to all samples processed with a PGMEA–alkane mixture. Examples are given for the 40/60 PGMEA–*n*-dodecane sample. (a) a cluster of solid spherical entities present on the surface of the film. Typical density of such entities is less than one small sphere per area shown in this micrograph; (b) top view of partially peeled surface. The pore-free skin has been preserved in the lower left portion of the micrograph. Typical skin thickness: 0.1–0.3 μm.

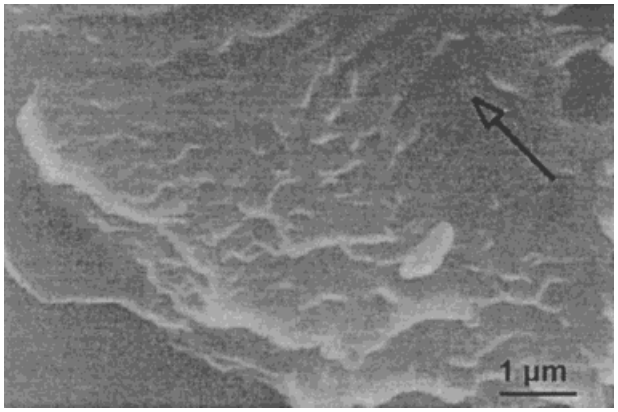

Figure 9 Side view of a liquid-nitrogen fractured film processed with a 20/80 MEK–*n*-decane (5 min soaking) and dried in the air. Arrow direction is perpendicular to the surface of the film.

3–4%. This lowering of density suggests the presence of undesirable density fluctuations in the bulk of the sample. These fluctuations may represent a collapsed intermediate PI structure of the soaking stage.

The air-dried 20/80 PGMEA–*n*-octane 3.95 μm sample showed a 6.5% loss and, in conformity to our expectations on the basis of volatility considerations, exhibited essentially no porosity.

In all Table II and III samples for which porosity was observed, the isolated pores with convex pore contours and small volume fractions suggest that PI took place during crossing of regime α. The existence of two pore-size families could correspond to different phase-separation stages.[2a] Nevertheless, as different pore sizes were found at different depths, the pore-size variation appears to reflect a variation in composition and phase-separation conditions with depth.

Although MEK is much more volatile than PGMEA, a liquid-nitrogen fractured sample processed with a 20/80 MEK–*n*-decane mixture showed a layeredlike fine structure but no clear signs of porosity (Fig. 9). This difference between PGMEA and MEK should be attributed to differences in the characteristics of the polymer–solvent–nonsolvent phase diagram. These characteristics include different locations of the binodal curve and T_g line. We may also note that although no pores could be observed, a modulation in density was present, as the impregnated sample was 10% thicker than the original layer. This modulation in density may well reflect a collapsed pore structure.

In the case of samples processed with the methanol–decane system, it must be noted that decane is not fully miscible with methanol. In addition, dissolution tests and the use of methanol as a nonsolvent for precipitation of the EPR fraction used in this work indicate that pure methanol at best swells the film resin. On the other hand, solubility parameter considerations[23] suggest that the EPR resin may lie roughly halfway between methanol and decane. Hence, for a range of λ values, single-phase soaking may proceed to a considerable depth before composition changes (during drying or during soaking plus drying) induce PI immiscibility. The observed high level of porosity (Figs. 10 and 11), very thin skins, and two coexisting families of pores (Fig. 11) are structural features similar to the ones found in the standard (e.g., cellulose acetate) PI membranes.[1,2] Hence, PI considerations pre-

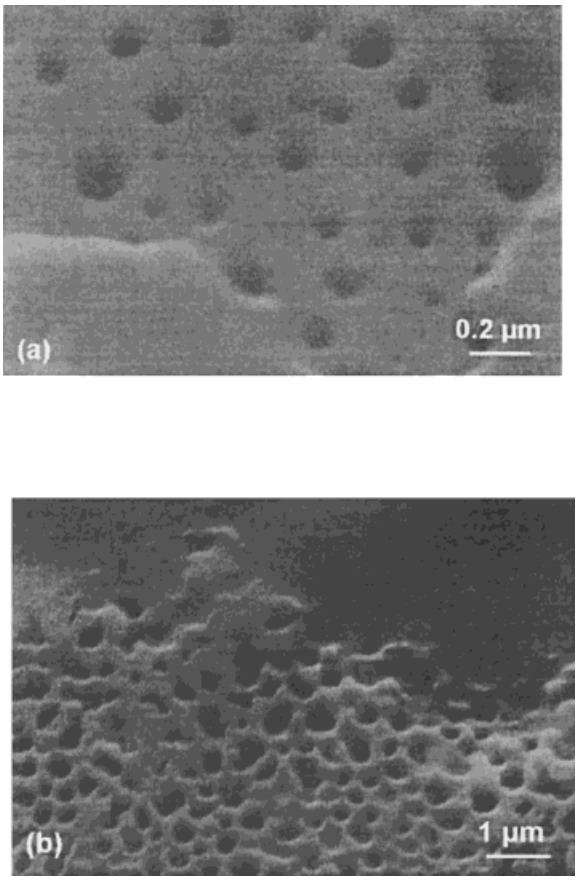

Figure 10 Morphology of films generated by soaking in a single phase 93.7/6.3 methanol–*n*-decane mixture. (a) Top view of a partially peeled top surface. (b) Top view of a fully peeled top surface, revealing a compact portion of the film under the porous layer. Taken together (a) and (b) suggest that the porous layer is sandwiched between two compact layers. See text for processing information.

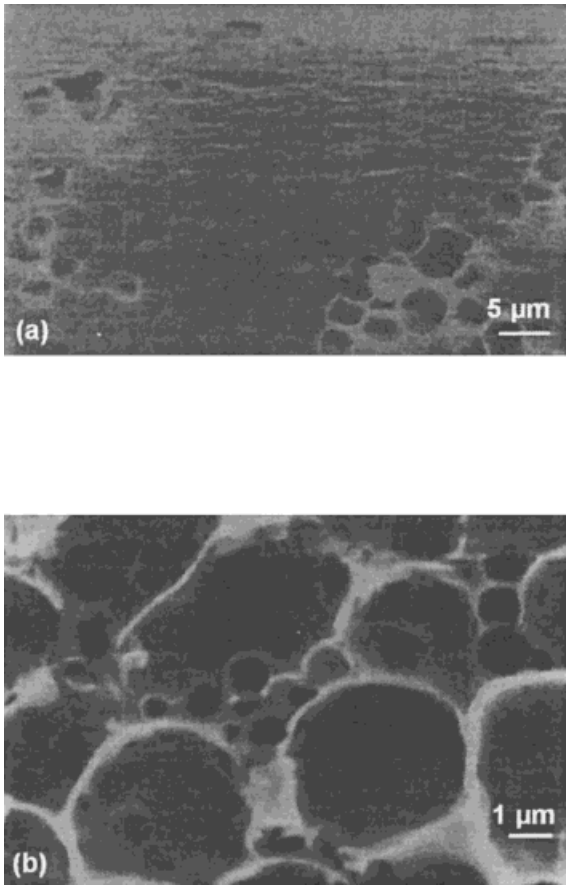

Figure 11 Morphology of films generated by soaking in a biphasic 20/80 methanol–*n*-decane mixture. (a) View of top surface. An occasionally peeled thin skin reveals an underlying porous structure. (b) Detail of a peeled top surface. Two distinct pore sizes are observed.

sented in Figure 2 may apply here as well, though the present situation is further complicated by the existence of a third immiscible pair (methanol–*n*-decane).

Our findings are pertinent to any solvent–nonsolvent postcasting processing of a noncrosslinked microelectronics film (or portion of film). We have demonstrated that PI structures can develop even for an original film thickness of 1.5 μm; in addition, the measured skin thickness (0.1–0.2 μm) and porous features observed at low depths suggest that, given the chance, PI effects can undermine a structure in the submicron range as well.

When poor film quality signs are noticed during wet processing, a shift toward a solvent–nonsolvent pair where the solvent is less volatile than the nonsolvent is the simplest solution to the problem of PI-related inhomogeneities. In a case where additional processing considerations impose severe restrictions on the choice of solvent and nonsolvent, still the variation of λ, x_o, processing time, and, if necessary, processing temperature can yield satisfactory structures. The λ value of choice will normally belong to regime II (or to the regime I–regime II border), and, in addition, the drying route should at best cross regime α, so that the generation of pores can be depressed rather effectively by quick drying. Such a depression is possible because NG phase separation starts in the form of fluctuations large in degree (occasional appearance of large composition gradients) but small in spatial extent; hence, and at early times (often on the order of 1 min for the systems of interest) the polymer solution may not nucleate at all. On the other hand, in the case of extensive crossing of regime γ, SD phase separation starts immediately in the form of fluctuations small in degree but large in extent; hence, while *large* compositional gradients may be prevented by quick drying, some type of inhomogeneity, such as a slight density-modulation, is harder to prevent.

In qualitative terms, it is expected that excessive volatility of the large nonsolvent λ values (for $\lambda < \lambda_T$), long soaking times and slow drying favor the formation of a film with a nondesirable PI structure. In addition, a second regime yielding undesirable porous structures may exist for very small λ values, if the T_g line cuts the binodal. In the latter case, accelerated drying can reduce but not eliminate porosity. For a nonsolvent that is moderately less volatile than the solvent (case of Table II data), a λ value lying between λ_T and λ_Λ (17/83 or the 14/86 compositions) satisfies simultaneously the requirement of low dissolution and low or zero porosity. This range of PGMEA–*n*-decane composition of soaking fluid compares well with the 15/85 to 15.8/84.2 ratio that was selected earlier[18a] on empirical grounds and for the purpose of satisfying a somewhat different set of processing requirements. It is also of interest that when the nonsolvent became much less volatile than the solvent (case of Table III data), there was no fully satisfactory combination of material loss and film porosity under slow-drying conditions. Nevertheless, fast drying is capable of nearly eliminating porosity for 20/80. and, thus, this composition would have been near satisfactory if *n*-dodecane were the preferred nonsolvent.

Finally, two points of general PI significance should be noted: (1) full PI structures can be

developed in films with a thickness of few microns, that is, films much thinner than standard asymmetric separation membranes; and (2) the molecular weight necessary to generate and support PI structures, including a skin, may even belong to the oligomeric range. Point (2) makes the ability to form and support a PI structure, one of the most lenient macromolecular character tests, in terms of minimum molecular-weight requirements.

CONCLUSIONS

1. Dry and wet PI phenomena are possible during processing of lithography resins.
2. Fine PI pore structure generated during drying following solvent–nonsolvent impregnation can be suppressed by choosing a less volatile solvent and/or a more volatile nonsolvent and/or by accelerated drying.
3. Control of a PI structure originating in the soaking period of a solvent–nonsolvent processing requires a combination of solvent–nonsolvent volatility, processing temperature, and time considerations.

The authors wish to acknowledge illuminating discussions with Drs. E. Gogolides and P. Argitis of IMEL Demokritos and also the help of Mr. A. Lapatas, Dr. S. Poulou, and Ms. E. Soterakou. A portion of this work was supported through funds from EPET II #724, Program of the Hellenic General Secretariat of Research and Development.

REFERENCES

1. Kesting, R. Synthetic Polymeric Membranes: A Structural Perspective, 2nd ed.; Wiley & Sons: New York, 1985.
2. (a) Beltsios, K.; Athanasiou, E.; Aidinis, K.; Kanellopoulos, N. J Macromol Sci, Phys Ed 1999, 38(1&2), 1; (b) Beltsios, K.; Bedard, M. C. J Macromol Sci, Phys Ed 2000, 39, 623.
3. Smolders, C. A.; Reuvers, A. J.; Boom, R. M.; Wienk, I. M. J Membr Sci 1992, 73, 259.
4. (a) Termonia, Y. J Polym Sci, Part B: Polym Phys 1995, 33, 279; (b) Termonia, Y. J Membr Sci 1995, 104, 173.
5. (a) Pinnau, I.; Koros, W. J. J Polym Sci Part B: Polym Phys 1993, 31, 419; (b) Pinnau, I.; Koros, W. J. J Appl Polym Sci 1991, 43, 1491.
6. Burghardt, W. R.; Yilmaz, L.; McHugh, A. J. Polymer 1987, 28, 2085.
7. Reuvers, A. J.; Altena, F. W.; Smolders, C. A. J Polm Sci: Part B: Polym Phys 1986, 24, 793.
8. (a) Tsiartas, P. C.; Flanangin, L. W.; Henderson, C. L.; Hinsberg, W. D.; Sanchez, I. C.; Bonnecaze, R. T.; Wilson, C. G. Macromolecules 1997, 30, 4656; (b) Peppas, N. A.; Wu, J. C.; von Meerwall, E. D. Macromolecules 1994, 27, 5626.
9. (a) Ueberreiter, K.; Asmussen, F. J Polym Sci 1962, 57, 187; (b) Asmussen, F.; Ueberreiter, K. J Polym Sci 1962, 57, 199.
10. (a) Gee, G. Trans Faraday Soc 1944, 40, 468; (b) Wolf, B. A.; Blaum, G. J Polym Sci, Polym Phys 1975, 13, 1115.
11. (a) Arnauts, J.; Berghmans, H. Polym Comm 1987, 28, 66; (b) Callister, S.; Keller, A.; Hikmet, Polymer 1988, 29, 1378.
12. (a) Lloyd, D. R.; Kinzer, K. E. J Membr Sci 1990, 52, 239; (b) Lloyd, D. R.; Kim, S. S.; Kinzer, K. E. J Membr Sci 1991, 64, 1.
13. (a) Burghardt, W. R. Macromolecules 1989; 22, 2482; (b) Smith, P.; Pennings, A. J. J Polym Sci, Polym Phys Ed 1977, 15, 523.
14. Beltsios, K.; Athanasiou, E.; Tegou, E.; Kougias, J.; Kanellopoulos, N. Phase Inversion Beyond Applications in Membrane Formation. II. Paints, Primers and Protective Coatings, manuscript in preparation.
15. Novembre, A. E.; Masakowski, L. M.; Hartney, M. A. Polym Eng Sci 1986, 26, 1158.
16. (a) Reiser, A.; Shih, H.-Y.; Yeh, T.-F.; Huang, J.-P. Angew Chem, Int Ed Engl 1996, 35, 2428; (b) Nonogaki, S.; Ueno, T.; Ito, T. Microlithography Fundamentals in Semiconductor Devices and Fabrication Technology; Marcel Dekker Inc.: New York, 1998; Chapter 4.
17. (a) Gogolides, E.; Tzevelekis, D.; Grigoropoulos, S.; Tegou, E.; Hatzakis, M. J Vac Sci Technol, B 1996, 14(5), 3332; (b) Hatzakis, M.; Shaw, J. M.; Stewart, K. J.; Peekskill, L. U.S. Pat. 5,041,358 (1991).
18. (a) Tegou, E.; Gogolides, E.; Argitis, P.; Boudouvis, A.; Hatzakis, M. Microelectron Eng 1998, 41/42, 335; (b) Tegou, E.; Goggolides, E.; Argitis, P.; Raptis, I.; Meneghini, G.; Cui, Z. Jpn J Appl Phys 1998, 37, 77; (c) Tegou, E.; Gogolides, E.; Hatzakis, M. Microelectron Eng 1997, 35, 141.
19. Argitis, P.; Raptis, I.; Aidinis, C. J.; Glezos, N.; Baciocchi, M.; Everett, J.; Hatzakis, M. J Vac Sci Technol 1995, B 13(6), 3030.
20. Strathmann, H.; Kock, K.; Amar, P.; Baker, R. W. Desalination 1975, 16, 179.
21. Hatzakis, M.; Stewart, K.; Shaw, J.; Rishton, S. J Electrochem Soc 1991, 138, 1076.
22. Zeman, L.; Frazer, T. J Membr Sci 1993, 84, 93.
23. Brandrup, J.; Immergut, E. H.; McDowell, W. Polymer Handbook, 2nd Ed.; Wiley & Sons: New York, 1975; Chapter IV.